metastable olivine (6, 7) and deep focus earthquakes through transformational faulting (26–28), and on mantle discontinuities (5), where nucleation kinetics can affect discontinuity thickness.

REFERENCES AND NOTES

1. D. L. Anderson, *Theory of the Earth* (Blackwell, Boston, 1989).
2. A. E. Ringwood, *Geochim. Cosmochim. Acta* **55**, 2083 (1991).
3. R. Jeanloz, *Geophys. Res. Lett.* **18**, 1743 (1991).
4. H. M. Benz and J. E. Vidale, *Nature* **365**, 147 (1993).
5. V. S. Solomatov and D. J. Stevenson, *Earth Planet. Sci. Lett.* **125**, 267 (1995).
6. C. M. Sung and R. G. Burns, *Tectonophysics* **31**, 1 (1976).
7. D. C. Rubie and C. R. Ross, *Phys. Earth Planet. Inter.* **86**, 223 (1994).
8. G. J. Wayte, R. H. Worden, D. C. Rubie, G. T. R. Droop, *Contrib. Mineral. Petrol.* **101**, 426 (1989).
9. D. C. Rubie, *Terra Abstr.* **7**, 113 (1995).
10. J. W. Christian, *The Theory of Phase Transformations in Metals and Alloys* (Pergamon, Oxford, 1965).
11. M. Liu and R. A. Yund, *Phys. Earth Planet. Inter.*, in press.
12. D. C. Rubie *et al.*, *J. Geophys. Res.* **95**, 15829 (1990).
13. B. R. Hacker, S. H. Kirby, S. R. Bohlen, *Science* **258**, 110 (1992).
14. The pressure medium for the experiments was a MgO octahedron with a 14-mm edge length, containing a stepped $LaCrO_3$ resistive heater [D. C. Rubie, S. Karato, H. Yan, H. St. C. O'Neill, *Phys. Chem. Miner.* **20**, 315 (1993)]. The assembly was compressed with Toshiba F-grade WC anvils with 8-mm truncations. The sample pressure was calibrated at 1473 K by reversing phase transitions in the SiO_2 and Mg_2SiO_4 systems, with a resulting uncertainty of approximately ±1 GPa. A contribution to the pressure uncertainty results from further pressurizing the sample at 873 K after hot pressing, a procedure that is different from the single-stage compression used for pressure calibration. Temperature was monitored with a W3%Re-W25%Re thermocouple without correction for the effect of pressure. The samples were loaded into 1.6-mm-diameter capsules and dried for several hours at 503 K in a vacuum oven before the experiments.
15. M. Akaogi, E. Ito, A. Navrotsky, *J. Geophys. Res.* **94**, 15663 (1989).
16. A. J. Brearley, D. C. Rubie, E. Ito, *Phys. Chem. Miner.* **18**, 343 (1992).
17. R. J. Angel, A. Chopelas, N. L. Ross, *Nature* **358**, 322 (1992). We refer to our Mg-rich clinopyroxenes as clinoenstatite in the quenched samples and as high clinoenstatite at transformation conditions.
18. R. Jeanloz and A. B. Thompson, *Rev. Geophys. Space Phys.* **21**, 51 (1983).
19. A. Hogrefe, D. C. Rubie, T. G. Sharp, F. Seifert, *Nature* **372**, 351 (1994).
20. Overprinted eclogite-grade rocks from the Bohemian Massif contain symplectites of orthopyroxene and hercynite spinel after garnet [P. J. O'Brien, *J. Metamorph. Geol.* **11**, 241 (1993)]. The orthopyroxene and spinel have the same crystallographic relation as that observed here (T. G. Sharp, unpublished results).
21. A. J. Brearley and D. C. Rubie, *Phys. Earth Planet. Inter.* **86**, 45 (1994).
22. D. C. Rubie and A. J. Brearley, *Nature* **348**, 628 (1990).
23. R. J. Angel and D. Hugh-Jones, *J. Geophys. Res.* **99**, 19777 (1994).
24. Y. Fei, S. K. Saxena, A. Navrotsky, *ibid.* **95**, 6915 (1990).
25. Y. Fei, H.-K Mao, J. Shu, *ibid.* **97**, 4489 (1992).
26. S. H. Kirby, W. B. Durham, L. A. Stern, *Science* **252**, 216 (1991).
27. P. C. Burnley, H. W. Green, D. J. Prior, *J. Geophys. Res.* **96**, 425 (1991).
28. H. W. Green and P. C. Burnley, *Nature* **341**, 733 (1989).

8 February 1995; accepted 19 May 1995

A Large Northern Hemisphere Terrestrial CO_2 Sink Indicated by the ^{13}C/^{12}C Ratio of Atmospheric CO_2

P. Ciais, P. P. Tans, M. Trolier, J. W. C. White,* R. J. Francey

Measurements of the concentrations and carbon-13/carbon-12 isotope ratios of atmospheric carbon dioxide can be used to quantify the net removal of carbon dioxide from the atmosphere by the oceans and terrestrial plants. A study of weekly samples from a global network of 43 sites defined the latitudinal and temporal patterns of the two carbon sinks. A strong terrestrial biospheric sink was found in the temperate latitudes of the Northern Hemisphere in 1992 and 1993, the magnitude of which is roughly half that of the global fossil fuel burning emissions for those years. The challenge now is to identify those processes that would cause the terrestrial biosphere to absorb carbon dioxide in such large quantities.

One of the most important problems in the science of global change is the balancing of the global budget for atmospheric CO_2. Although anthropogenic activities have clearly altered the global carbon cycle, significant gaps exist in our understanding of this cycle. Of the CO_2 emitted into the atmosphere as a result of burning fossil fuels, roughly half remains in the atmosphere and the other half is absorbed into the oceans and the terrestrial biosphere. The partitioning between these two sinks is the subject of considerable debate. Whereas most chemical oceanographers are confident that the oceanic sink is not large enough to account for the entire absorption, many terrestrial ecologists doubt that the land biosphere can be a large carbon sink, particularly given the source to the atmosphere through deforestation, hence, the issue of the "missing" carbon sink. Without a good accounting for the fate of CO_2 leaving the atmosphere, predictions of future CO_2 concentrations that result from different emission scenarios will remain uncertain. This, in turn, weakens the link between energy policy and climate change.

Observations of the north-south gradient of atmospheric CO_2 show that there must be a large carbon sink in the Northern Hemisphere (1, 2). This sink has been ascribed either to the North Atlantic Ocean, on the basis of sparse measurements of ^{13}C/^{12}C ratios in atmospheric CO_2 (1), or to terrestrial mechanisms, on the basis of measurements of the saturation of surface seawater with respect to atmospheric CO_2 (2). The latter study disagreed with the former and suggested that it is unlikely that the northern oceans could be responsible for most of the sink. Here we present the results of a greatly expanded global network of measurements of ^{13}C/^{12}C ratios in atmospheric CO_2. The ^{13}C/^{12}C ratios provide a good fingerprint of terrestrial biospheric fluxes of CO_2, as plant photosynthesis discriminates against ^{13}C, whereas isotopic fractionation during CO_2 invasion into the oceans is small. Thus, in combination with concentration measurements, ^{13}C/^{12}C ratios can be used to distinguish the oceanic and terrestrial biospheric fluxes of CO_2 from the atmosphere. Our results for 1992 and 1993 indicate that a strong terrestrial biospheric carbon sink existed in the temperate latitudes of the Northern Hemisphere during those years with a magnitude roughly half that of the global fossil fuel burning flux.

Since 1990, the Stable Isotope Laboratory at the Institute of Arctic and Alpine Research (INSTAAR) has measured δ^{13}C (3) in CO_2 from weekly samples of air from a network of sites, complementing measurements of CO_2 mixing ratios made by the National Oceanic and Atmospheric Administration's Climate Monitoring and Diagnostics Laboratory (NOAA/CMDL). In 1992 and 1993, 41 sites from this network were measured for δ^{13}C. These data were augmented by measurements made by the Commonwealth Scientific and Industrial Research Organisation (CSIRO) from two sites (4) at high southern latitudes (Fig. 1). From the smoothed atmospheric observations, the latitudinal distribution of the sur-

P. Ciais, National Oceanic and Atmospheric Administration's Climate Monitoring and Diagnostics Laboratory (NOAA/CMDL), R/E/CG1, 325 Broadway, Boulder, CO 80303, USA, and LMCE-DSM Commissariat a l'Energie Atomique, L'Orme des Meurisiers, 91191, Gif sur Yvette Cedex, France.
P. P. Tans, NOAA/CMDL, R/E/CG1, 325 Broadway, Boulder, CO 80303, USA.
M. Trolier, NOAA/CMDL, R/E/CG1, 325 Broadway, Boulder, CO 80303, USA, and Institute of Arctic and Alpine Research (INSTAAR), University of Colorado, Boulder, CO 80309, USA.
J. W. C. White, INSTAAR, and Department of Geological Sciences, University of Colorado, Boulder, CO 80309, USA.
R. J. Francey, Commonwealth Scientific and Industrial Research Organisation, Division of Atmospheric Research, Mordialloc, Victoria 3195, Australia.

---

*To whom correspondence should be addressed.

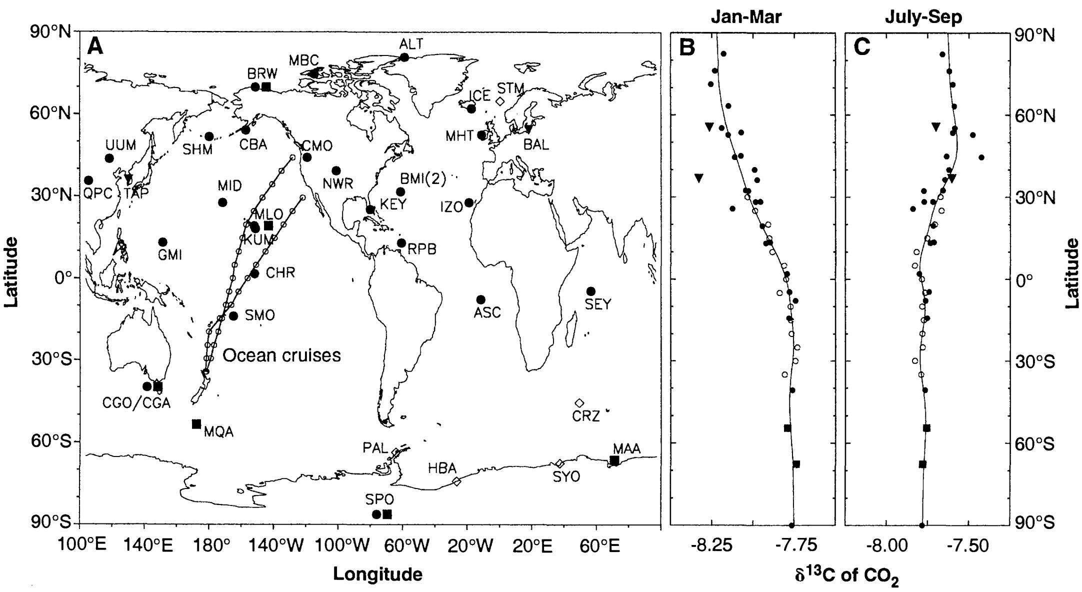

Fig. 1. (**A**) Map of the global network of sites where air samples are collected weekly for measurement of $\delta^{13}C$ and CO_2. ●, NOAA–University of Colorado sites measured for CO_2 and $\delta^{13}C$; ○, NOAA–University of Colorado shipboard data measured for CO_2 and $\delta^{13}C$; ◇, NOAA sites measured only for CO_2; ■, CSIRO sites; ▼, "polluted" sites close to large industrial areas (TAP, BAL) where the atmosphere is typically more depleted in $^{13}CO_2$ and has a higher CO_2 partial pressure (p_{CO_2}) than the latitudinal average. The "polluted" sites are kept in the latitudinal fit but are given a smaller weight. (**B**) Observed north-south gradients of $\delta^{13}C$ in the atmosphere in 1993 in winter (January to March) and (**C**) in summer (July to September). The fit to the observations (solid line) is constructed in the same manner as the quasi-weekly fits used in the inverse model.

face fluxes of CO_2 and $^{13}CO_2$ have been calculated, with mass conservation, by using a two-dimensional (latitude, height) zonally averaged model of atmospheric transport (*5*, *6*). This "inverse" method is constrained at Earth's surface at every latitude and time step by the atmospheric observations, yielding mathematically unique solutions for the separate fluxes of CO_2 and $^{13}CO_2$. The partitioning of the net fluxes from land and oceans is then determined from linear equations (*6*). We note that surface fluxes calculated in this way do not entirely equate to storage in the same region, as some of the carbon fixed by photosynthesis on land finds its way to the oceans via rivers or escapes in the form of reduced gases such as CO, CH_4, and other hydrocarbons (*7*).

Apart from known fossil fuel emissions and their isotopic composition (*8*), the procedure depends on three parameters [for details see (*6*)]. First, the discrimination against ^{13}C by plant photosynthesis, linked to the partial pressure of CO_2 (p_{CO_2}) in chloroplasts (*9*), is calculated monthly from the coupled biosphere model, SiB-2 (*10*, *11*). The SiB-2 model has a resolution of 4° by 5° and is coupled to the Colorado State University general circulation model. With SiB-2 the full carbon and water budgets of plants can be explicitly and interactively calculated (*12*). This approach has the advantage that monthly averages are calculated from detailed diurnal cycles of the pertinent variables, thus capturing the effects of processes on all relevant time scales. Our discrimination model makes a distinction between C_4 and C_3 plants on a geographical basis, but it does not account for seasonal asynchrony between the two fixation pathways in mixed ecosystems.

Second, the isotopic composition of carbon respired by soils is calculated with the CENTURY soil model (*13*). Organic carbon in soils derives from the products of photosynthesis of previous years (when the atmospheric $\delta^{13}C$ was less negative than it is today as the result of the addition of CO_2 from fossil fuels depleted in ^{13}C). In the global version of the CENTURY model, soil organic carbon is divided into four sep-

Table 1. Ocean and land exchange of CO_2 averaged over large latitude bands with the corresponding error estimates. Ocean and land fluxes bear identical uncertainties but correlate such that the sum of ocean and land fluxes always equals the net flux of CO_2 (the latter is expressed after subtraction of fossil fuels). The uncertainties of each of the isotopic parameters (given in the lower part of the table) were estimated as follows: the disequilibrium of carbon in soils is uncertain by 30%, the photosynthetic fractionation by 1 per mil, $\delta^{13}C$ of carbon in surface waters by 0.2 per mil, and the air-sea gas exchange by 30%. For the variation in longitude of CO_2 and $\delta^{13}C$ observations, we made repeated runs of the two-dimensional model (*5*, *6*) using different bootstrap selections of the sites shown in Fig. 1. The uncertainty in the magnitude and isotopic labeling of fossil fuel releases do not have a large effect on the deduced partitioning between ocean and land. For example, a mismatch of 1 per mil between the estimated and real values of $\delta^{13}C$ in fossil fuels would lead to an error on the estimated global terrestrial uptake of only 25 Tmol of CO_2 (0.3 gigatons of C) (*6*, *24*). Eq, equator.

Area isotopic parameters	Partitioning of CO_2 by latitude band (Tmol of CO_2)						
	90°N–30°S	30°S–Eq	Eq–30°N	30°N–90°N	Global	Fossil fuel emissions	Atmospheric increase
	Partitioning of CO_2 in 1992						
Land	−46	−33	244	−354	−190		
Ocean	−95	19	−101	−27	−205		
Total	−141	−14	143	−382	−394	508	114
	Partitioning of CO_2 in 1993						
Land	−65	−26	97	−253	−246		
Ocean	−77	65	−33	−55	−99		
Total	−142	39	65	−307	−345	508	163
	Uncertainty estimates of CO_2 partitioning						
Isotopic parameters							
Disequilibrium with soils	0	4	3	7	9		
Disequilibrium with oceans	28	24	20	10	44		
Discrimination by photosynthesis	5	4	4	12	14		
Longitudinal variability	20	30	55	43	75		
Total uncertainty	35	39	59	46	89		

arate pools in which the residence time of carbon is controlled by temperature and soil texture. As an example, 20% of the carbon respired at high northern latitudes is found to lag the atmosphere by up to 100 years. In forest ecosystems, the residence time of carbon in soils is augmented to account for previous storage in aboveground woody tissues. We assumed that woody tissues make up about 30% of the total aboveground biomass and that they lag the atmosphere by 40 years on average.

Third, the $\delta^{13}C$ of ocean surface waters, which also lags the decrease forced on the atmosphere, is estimated from a compilation of measurements (*14*). The influence on the atmosphere is modulated by the air-sea transfer velocity (*15*).

We also estimated how systematic errors in these three parameters affect our conclusions by letting each one vary about its preferred value (*16*). The longitudinal variations of the data contribute to the uncertainty of our results from the two-dimensional model. We partially evaluate this through a bootstrap analysis, where the land-ocean partitioning is repeatedly calculated after adding and omitting measurement sites. This method also yields an estimate of the error due to sparse data coverage. The estimates of the above sources of error are summarized in Table 1.

At this time, we can draw conclusions about the nature of strong regional CO_2 fluxes, though not yet about the precise globally integrated partitioning between land and oceans. The global total land and ocean fluxes are sums of positive and negative regional contributions; the relative magnitude of their sums is sensitive to assumptions about the time lag in the propagation of an atmospheric isotopic signature into the terrestrial biosphere and to the absolute calibration of the isotopic measurements. The uncertainty of the isotopic equilibrium fractionation factor between CO_2 in the atmosphere and in ocean water also contributes significantly (*17*). However, on a regional scale, such uncertainties can be overwhelmed by the large size of the fluxes, as is the case for the biospheric sink we infer between 30°N and 60°N.

The annual mean oceanic and terrestrial CO_2 fluxes are plotted as a function of latitude in Fig. 2. There is a major sink on land between 30°N and 60°N prevailing from June to September (Fig. 3). Over the past 2 years, this sink has averaged 290 Tmol (10^{12} mol) of CO_2 per year, which is equivalent to 3.5 gigatons of carbon (*18*) or more than half of the total global fossil fuel burning flux for those years. This is about 200 Tmol more than the regrowth estimated from forest inventory studies (*19*). There are several possible explanations for this large carbon sink in the terrestrial biosphere. Our result might be a preliminary indication that, in addition to regrowth of forests, nutrient fertilization or CO_2 fertilization (or both) of temperate and sub-boreal ecosystems is now occurring. Alternatively, climatic differences between 1992–1993 and the previous decade may have altered the balance of photosynthesis and respiration in this area. Finally, this sink may not be a recent phenomenon but may have been present for decades.

The study by Keeling and co-workers (*1*) also made use of CO_2 and $\delta^{13}C$ data, but they came to the opposite conclusion that the CO_2 sink in the Northern Hemisphere had to be mostly oceanic. Their analysis relied much less on spatial gradients than ours. The strongest constraint in their analysis was a box model of the carbon cycle to keep track of the decadal mass balances of CO_2 and $\delta^{13}C$. After making some assumptions about geographical aspects of the operation of the carbon cycle, they compared their calculated spatial distributions of CO_2 and $\delta^{13}C$ with observations as a consistency check. Our method relies primarily on the spatial distributions of concentrations and isotopes of recent years, and our conclusions are therefore limited strictly to 1992 and 1993.

A small part of the difference between the conclusions of this study and those of Keeling and co-workers can be attributed to the fact that their method, that is, the box model, is based on the storage of carbon, whereas ours detects only CO_2 fluxes to and from the atmosphere and not carbon transport in rivers or in the atmosphere by species other than CO_2 (*7*). We believe that a larger part of the difference is explained by our much greater data density. For 1992 and 1993, a larger net annual uptake of CO_2 (~100 Tmol) is inferred for the 30°N to 60°N terrestrial biospheric sink when our full network of measurement sites are used for calculations than when only the six sites

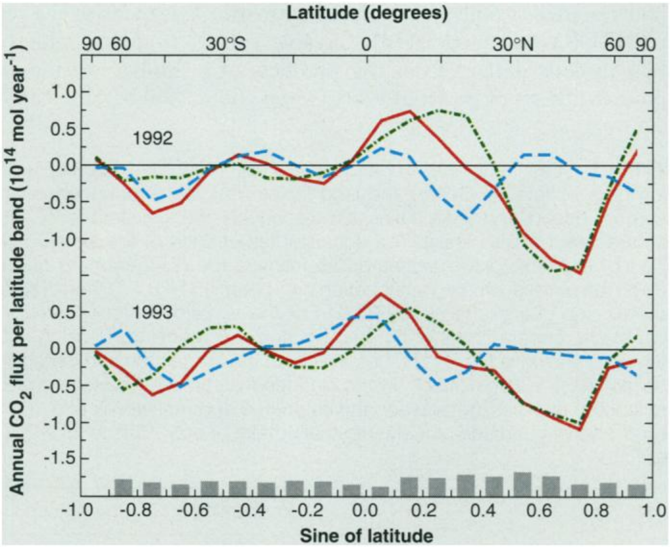

Fig. 2. Ocean and land partitioning of CO_2 as a function of latitude. The solid red line is the annual mean net flux of CO_2 without the contribution of fossil fuel emissions. The dashed blue line is the net exchange of CO_2 with the oceans, and the dash-dot green line is the net exchange on land. Units are 10^{14} mol of CO_2 per year (100 Tmol $year^{-1}$) for each model latitude band. The model has 20 equal area bands in sine of latitude. The errors (one-sided, 1σ) are plotted on the bottom axis for each latitude band.

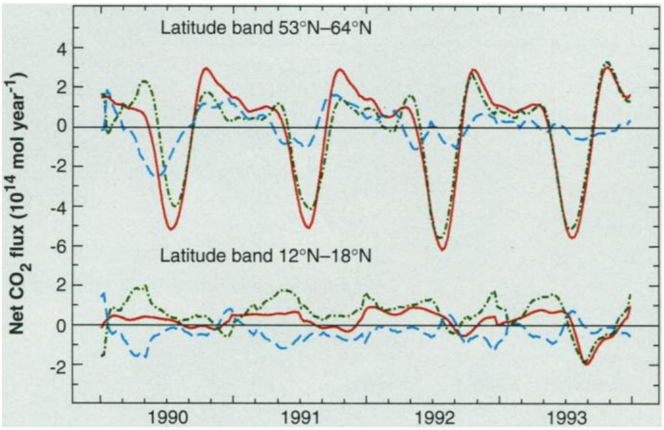

Fig. 3. Ocean and land partitioning of CO_2 fluxes as a function of time. Latitude bands in the tropics and at northern mid-latitudes are shown as examples. At northern mid-latitudes, the lower values for net growing season uptake during 1990 and 1991 are artifacts of the sparser isotopic measurements in those years. When constrained with sufficient data, the seasonality of carbon uptake in the tropics is clearly terrestrial. We note that the mirroring effect of the terrestrial biospheric and oceanic fluxes for the tropical zone may be indicative of a problem with the isotopic data (see text). The colored lines are as described in Fig. 2.

are used for which we have $\delta^{13}C$ time series in 1990 and 1991. It is also possible that part of the difference lies in the substantial temporal variability in the terrestrial and oceanic carbon sinks inferred from the Keeling isotope data compared with that from a long isotope record from Cape Grim by Francey and co-workers (*20*). Although there is no doubt about the existence of interannual variability in sources and sinks, the results of Francey *et al.* exhibit substantially less interannual variation than those of Keeling *et al.*, possibly because of calibration differences. The present results are in general agreement with the earlier work by Tans *et al.* (*2*), in which they used atmospheric CO_2 data of 1981 to 1987 and a compilation of p_{CO_2} measurements of the surface oceans made from 1972 to 1989.

Despite our confidence that the above sink is real, there is still ample room for improvement in this technique for estimating carbon fluxes. For example, the oceans north of 10°N appear to have taken up CO_2 at an average rate of 150 Tmol $year^{-1}$ during 1992 and 1993. Most of this was in the latitude band from 10°N to 25°N. This is not substantiated by observations of the difference in p_{CO_2} between ocean surface water and the atmosphere (*2, 21*). We do not know the exact cause of this discrepancy. It could be due to the allocation of carbon between C_3 and C_4 plants at these latitudes. Uptake and loss of carbon by C_4 plants is almost indistinguishable isotopically from ocean uptake. Thus, if deforestation is predominantly from C_3 plants (trees), then we have overestimated the terrestrial source of carbon in the model by ascribing some carbon in these latitudes to C_4 plants (grasses). This problem is worsened if C_4 grasses replace C_3 trees after deforestation. It is also possible that a small offset between the $\delta^{13}C$ values measured in flasks taken from ships and flasks taken at the island sites may exist (*22*). The offset in the isotopic data appears to be smaller in 1993 than in 1992, which is consistent with the smaller oceanic sink inferred in 1993. Both of these potential problems affect the deconvolution between 20°S and 20°N most, where shipboard data dominate and C_4 plants are more abundant. Regardless of the source of the discrepancy between our deconvoluted oceanic sink and the oceanic data, the inverse relation between the oceanic sink and the terrestrial source between 10°N and 25°N raises a caution flag (*20*). Such a relation is expected if problems exist in the measuring or modeling of the isotopic data.

Land areas in the northern tropics and subtropics appear to be a net source of CO_2 to the atmosphere (100 to 200 Tmol $year^{-1}$) from January to July, possibly associated with the seasonal burning of African savannas (*23*), although the discussion above suggests that the terrestrial sources may be overestimated. In the southern tropics, CO_2 is released to the atmosphere from September to December, though there is no significant annual mean source of CO_2. In fact, applying the same arguments made above about C_4 plants and uncertainty in shipboard data would result in a terrestrial sink in the southern tropics. This may suggest that the ongoing net deforestation in Southeast Asia and the Amazon is currently overestimated, or that it is offset by regrowth or fertilization of tropical forests.

We find that zonally averaged equatorial oceans are outgassing CO_2 at a rate of at least 70 Tmol $year^{-1}$ without a clear seasonality. The oceans south of 20°S are a net sink of CO_2. Note that in 1993 we infer a residual sink on land near 50°S, which is unlikely given the lack of land at this latitude. The problem may be caused by interannual and seasonal variability of the $^{13}C/^{12}C$ ratio in southern ocean surface waters, not easily accounted for with the current paramaterizations used in our model, and possibly contributed to by sparse data coverage in the far southern latitudes. We note that these problems are most troublesome in the high southern latitudes and do not seriously affect our conclusion of a strong terrestrial sink in the Northern Hemisphere.

Errors potentially arising from the treatment of intrahemispheric atmospheric transport in our model remain to be better quantified. If such transport were weaker in our model than in the real world, then CO_2 originating from ^{13}C-depleted fossil fuel would not be sufficiently dispersed within the modeled Northern Hemisphere, leading to an overestimate of the land sink at the latitudes of greatest fossil fuel emissions. This point can be addressed by comparing different models, as well as by the use of new tracers of atmospheric circulation such as SF_6.

The main purpose of the international effort to monitor atmospheric CO_2 and its isotopic ratios is to characterize the present-day carbon cycle. The observations of large-scale sources and sinks must form the underpinning of our understanding of the carbon cycle and therefore of the predictions of the future CO_2 loading of the atmosphere. Although the large sink in the terrestrial biosphere identified in this study may be natural, the possibility that it is anthropogenically induced (for example, by nitrogen or CO_2 fertilization effects on Russian boreal forests or regrowth of forests in North America) raises important questions. Because carbon storage on land is likely to be more transient and vulnerable to anthropogenic and climatic perturbations than storage in the oceans, the current partitioning of CO_2 uptake between the oceans and the land biosphere may well have significant implications for future increases in atmospheric CO_2.

REFERENCES AND NOTES

1. C. D. Keeling, S. C. Piper, M. Heimann, in *Aspects of Climate Variability in the Pacific and Western Americas*, D. H. Peterson, Ed. (American Geophysical Union, Washington, DC, 1989), vol. 55, p. 165.
2. P. P. Tans, I. Y. Fung, T. Takahashi, *Science* **247**, 1431 (1990).
3. A measurement of $\delta^{13}C$ is calculated as follows:

$$\delta^{13}C_{\mathrm{sample}} = \left[\frac{(^{13}C/^{12}C)_{\mathrm{sample}}}{(^{13}C/^{12}C)_{\mathrm{standard}}} - 1\right]1000$$

the standard is PDB-CO_2 {CO_2 gas evolved from the carbonate PeeDee Belemnite (PDB) by reaction with phosphoric acid at 25°C [H. Craig, *Geochim. Cosmochim. Acta.* **12**, 133 (1957)]}.
4. The CSIRO sites are SPO, CGA, MQA, MAA, MLO, and BRW on Fig. 1. MQA and MAA are unique to CSIRO.
5. P. Tans, T. J. Conway, T. Nakazawa, *J. Geophys. Res.* **94**, 5151 (1989).
6. P. Ciais *et al.*, *ibid.* **100**, 5051 (1995).
7. I. G. Enting and J. V. Mansbridge, *Tellus* **B43**, 156 (1991); J. Sarmiento and E. T. Sundquist, *Nature* **356**, 589 (1992); P. P. Tans, I. Y. Fung, I. G. Enting, in *Biotic Feedbacks in the Global Climate System*, G. M. Woodwell and F. T. Mackenzie, Eds. (Oxford Univ. Press, London, 1995), p. 351.
8. T. Boden, personal communication [cited in R. J. Andres, G. Marland, T. Boden, S. Bishoff, in *The Carbon Cycle*, T. M. Wigley and D. Schimel, Eds. (Cambridge Univ. Press, Stanford, CA, in press)].
9. G. D. Farquhar, J. R. Ehleringer, K. T. Hubick, *Annu. Rev. Plant Physiol.* **40**, 503 (1989).
10. P. J. Sellers, J. A. Berry, G. J. Collatz, C. B. Field, F. G. Hall, *Remote Sens. Environ.* **42**, 187 (1992).
11. G. J. Collatz, J. T. Ball, C. Grivet, J. A. Berry, *Agric. For. Meteorol.* **54**, 107 (1991).
12. A. S. Denning, thesis, Colorado State University, Fort Collins, CO, (1994).
13. D. S. Schimel *et al.*, *Global Biogeochem. Cycles* **8**, 279 (1994).
14. We compiled $\delta^{13}C$ measurements in surface waters using ship transects in the Indian and Pacific oceans [R. Francois *et al.*, *ibid.* **7**, 627 (1993); P. D. Quay, B. Tilbrook, C. S. Wong, *Science* **256**, 74 (1992)] and using GEOSECS measurements in the Atlantic, adjusted for by a decreasing trend of 0.01 per mil every year [*GEOSECS, Atlantic, Pacific and Indian Ocean Expeditions, Vol. 7, Shorebased Data and Graphics* (National Science Foundation, Washington, DC, 1987)]. We do not account for seasonal variations of $\delta^{13}C$ in the surface ocean.
15. The variation in time and space of the CO_2 air-sea gas exchange velocity used to estimate fluxes from Δp_{CO_2} (the difference in p_{CO_2}) is derived from satellite wind speed and sea surface temperature measurements between 1990 and 1993 [J. Etcheto, J. Boutin, L. Merlivat, *Tellus* **B43**, 247 (1991)]. For 1992 and 1993, the gas exchange velocity fields have been analyzed on the basis of the SSM/I satellite observations. The formulation of Liss and Merlivat [P. S. Liss and L. Merlivat, in *The Role of Air-Sea Exchange in Geochemical Cycling*, P. Buat-Menard, Ed. (Reidel, Norwell, MA, 1986), p. 113] is scaled by a factor of 1.6, to make it compatible with bomb ^{14}C.
16. P. Ciais, R. J. Francey, P. P. Tans, J. W. C. White, M. Trolier, *NOAA Technical Memorandum ERL-CMDL-8*, in press.
17. P. P. Tans, J. A. Berry, R. F. Keeling, *Global Biogeochem. Cycles* **7**, 353 (1993).
18. One-hundred Tmol of CO_2 is equivalent to 1.2 gigatons of carbon. We prefer mole units because there is no confusion about the species considered.
19. R. K. Dixon *et al.*, *Science* **263**, 185 (1994).
20. R. J. Francey *et al.*, *Nature* **373**, 326 (1995).
21. For the North Atlantic Ocean, T. Takahashi, T. T. Takahashi, S. C. Sutherland, *Trans. R. Soc. London, Ser. B*, in press; for the North Pacific Ocean, T. T. Takahashi, personal communication.
22. Air samples at most sites are obtained by flushing

glass flasks that have been prefilled and shipped with clean, dry air. For the ships, evacuated flasks are exposed to air. Potential offsets between these two sampling methods are still under investigation.

23. P. J. Crutzen and M. O. Andreae, *Science* **250**, 1669 (1990). The burning of savannas in North Africa occurs essentially from December to March. It could be followed by the decomposition of organic matter in soils during the next rain season from April to July (H. Cachier, personal communication).
24. F. Joos, P. Ciais, L. Currie, in "Isotope Variation of Carbon Dioxide and Other Trace Gases in the Atmosphere," K. Rozanski, Ed. [final report on the International Atomic Energy Agency (IAEA) Coordinated Research Program, IAEA, Vienna, Austria, 1995].
25. We thank P. Gemery, D. Young, C. Brock, D. Bryant, D. Decker, and S. Webb for making the isotopic analyses. T. Conway and N. Zhang were responsible for the analyses of CO_2 and L. Waterman for the logistics of the flask network. We are grateful to the many individuals and organizations who contributed to the NOAA/CMDL cooperative flask sampling network. The Cape Grim Baseline Air Pollution Station, the Australian Antarctic Division, and CSIRO's GASLAB assisted in the provision of Southern Hemisphere results. K. Masarie contributed to the data management of $\delta^{13}C$. Partial support was provided by the Ocean Atmosphere Carbon Exchange Study and the Atmospheric Chemistry projects of the Climate and Global Change Program of NOAA and by the Atmospheric Research and Exposure Assessment Laboratory of the Environmental Protection Agency.

13 February 1995; accepted 12 June 1995

Similarity of *sli-1*, a Regulator of Vulval Development in *C. elegans*, to the Mammalian Proto-Oncogene *c-cbl*

Charles H. Yoon, Junho Lee, Gregg D. Jongeward,
Paul W. Sternberg*

Vulval induction during *Caenorhabditis elegans* development is mediated by LET-23, a homolog of the mammalian epidermal growth factor receptor tyrosine kinase. The *sli-1* gene is a negative regulator of LET-23 and is shown here to encode a protein similar to c-Cbl, a mammalian proto-oncoprotein. SLI-1 and c-Cbl share approximately 55 percent amino acid identity over a stretch of 390 residues, which includes a C_3HC_4 zinc-binding motif known as the RING finger, and multiple consensus binding sites for Src homology 3 (SH3) domains. SLI-1 and c-Cbl may define a new class of proteins that modify receptor tyrosine kinase–mediated signal transduction.

The induction of the vulva in *Caenorhabditis elegans* provides a model system in which to apply genetic analysis in order to dissect proto-oncogene function (*1*). Vulval induction is mediated by LET-23, a homolog of the epidermal growth factor receptor tyrosine kinase; by SEM-5, a Grb2-like adaptor; and by LET-60, a Ras protein (*2–4*). Genetic analyses have identified negative regulators of this pathway. Thus, the *sli-1* (suppressor of lineage defect) locus was defined by extragenic suppressors of *let-23* reduction-of-function (*rf*) mutations (*5*). The *let-23(rf)* mutations cause at least five phenotypes: defects in (i) viability, (ii) hermaphrodite fertility, (iii) male spicule development, (iv) posterior epidermal development, and (v) vulval differentiation (*6*). The *sli-1(rf)* mutations suppress all known defects of *let-23(rf)* mutations with the exception of sterility. For example, the *sli-1(sy143)* mutation restores vulval induction to wild type in animals with *let-23(sy97)*, a severe reduction-of-function allele that truncates a part of the LET-23 cytoplasmic tail and results in a vulvaless (Vul) phenotype (*6*). *sli-1* does not, however, bypass the requirement for *let-23* because *sli-1(rf)* mutations do not suppress *let-23* null alleles, which are lethal.

Reduction-of-function mutations in *sem-5* and *let-60* also display Vul phenotypes, and the products of these genes act downstream in a signal transduction process initiated by LET-23 (*3, 4*). The *sli-1(sy143)* mutation suppresses the Vul phenotype associated with a weakly hypomorphic *sem-5(n2019)* to near, but not greater than, wild type; *sli-1(sy143)* also weakly suppresses a very weak *let-60(rf)* mutation, *n2021* (*5*). Lethality associated with *let-60(s1124)*, a severe hypomorph, is not suppressed by *sli-1(sy143)* (*5*), which suggests that the *sli-1(rf)* mutation does not bypass the requirement for LET-60.

Although *sli-1(rf)* mutations alone are silent in a *let-23(+)* background, in combination with a mutation in another silent negative regulator of LET-23–mediated vulval development, *unc-101*, a *sli-1(rf)* mutation displays a multivulva (Muv) phenotype (*7*). Therefore, SLI-1 can act on signaling by wild-type LET-23.

We have now identified *sli-1* at the molecular level by positional cloning. Three-factor mapping positioned *sli-1* midway between *egl-17* and *unc-1*, which are about one map unit apart on the extreme left end of the *C. elegans* X chromosome (Fig. 1A) (*5*). The restriction fragment length polymorphism (RFLP) *stP41* links the genetic and physical maps in this region: *stP41* is tightly linked to *unc-1* and thus defines the right boundary of our region of interest (*8*). Assuming that the left boundary is the left end of the X chromosome, *sli-1* lies in the middle of a region spanned by $\sim$40 cosmids (*9*). To assay for *sli-1(+)* wild-type activity, we used a sensitive vulva-specific *let-23(rf)* allele, *sy1*. Whereas *let-23(sy1)* is Vul (Fig. 2B), *let-23(sy1); sli-1(sy143)* animals have a Muv phenotype (Fig. 2C). We microinjected candidate cosmids from the middle of the genomic region of interest into the germ line of the *let-23(sy1); sli-1(sy143)* parental strain and observed the vulval phenotype of stably transformed progeny in F_2 or later generations (*10*). Microinjection of the cosmid T18D5 rescued the Muv phenotype of *let-23(sy1); sli-1(sy143)* double mutants, and stable germ line–transformed progeny showed the Vul phenotype typical of *let-23(sy1)* strains (Fig. 1A and Fig. 2, B and D). Other cosmids in the region (F02G3, F25H6, and F25E2) did not rescue the Muv phenotype of the *let-23(sy1); sli-1(sy143)* parent strain. T18D5 also rescued the Muv phenotype of another *sli-1* allele, *sy129*, in our assay, which indicates that this cosmid contains the wild-type activity of *sli-1*.

We tested subclones of the 35-kb genomic insert of T18D5 to localize the region responsible for rescuing activity. A 16-kb Eco RV–Nhe I subclone (pSli1.16) and a 10-kb Eco RV–Nhe I subclone (pSli1.10) retained the rescuing activity of T18D5 (Fig. 1B and Table 1). Thus, these two subclones contain the wild-type *sli-1* gene; the smaller pSli1.10 is contained within the larger pSli1.16.

We isolated complementary DNAs (cDNAs) by probing the Barstead cDNA library with a 9-kb genomic fragment that overlaps pSli1.10 (*11*). One cDNA was 2.2 kb in length and is likely to be full length, because it includes the last nine base pairs of the SL1 trans-spliced leader sequence at the 5′ end. We also identified one class of alternatively spliced cDNA. We sequenced the full-length 2.2-kb cDNA, the longest available alternatively spliced cDNA, and the genomic fragment in pSli1.10. The open reading frame of the 2.2-kb cDNA encodes a putative translation product of 582 amino acids. The genomic structure of *sli-1* consists of 11 exons and 10 introns, spanning 6 kb in

---

C. H. Yoon and P. W. Sternberg, Howard Hughes Medical Institute and Division of Biology, California Institute of Technology, Pasadena, CA 91125, USA.
J. Lee, Department of Molecular and Cell Biology, University of California, Berkeley, CA 94720, USA.
G. D. Jongeward, Department of Microbiology, Immunology, and Biochemistry, University of California, San Francisco, CA 94143–0502, USA.

*To whom correspondence should be addressed.